Chemical Engineering Journal 160 (2010) 378–382

Contents lists available at ScienceDirect

Chemical Engineering Journal

journal homepage: www.elsevier.com/locate/cej

Preparation, characterization and antimicrobial activities of chitosan/Ag/ZnO blend films

Li-Hua Li, Jian-Cheng Deng*, Hui-Ren Deng, Zi-Ling Liu, Xiao-Li Li

College of Chemistry, Xiangtan University, Key Laboratory of Environmentally Friendly Chemistry and Applications of Ministry of Education, Xiangtan 411105, Hunan, China

ARTICLE INFO

Article history:
Received 13 December 2009
Received in revised form 13 March 2010
Accepted 19 March 2010

Keywords:
Chitosan
ZnO
Ag
Nanoparticles
Antimicrobial activities
Blend films

ABSTRACT

Novel chitosan/Ag/ZnO (CS/Ag/ZnO) blend films were prepared via a new method of sol-cast transformation. The blend films were characterized by UV–vis absorption spectroscopy (UV–vis), X-ray diffraction (XRD), scanning electron microscopy (SEM), transmission electron microscopy (TEM) and Energy Dispersive X-Ray Fluorescence Spectrometry (EDX). The results revealed that ZnO and Ag nanoparticles (NPs) with spherical and granular morphology had uniform distribution within chitosan polymer. The product had excellent antimicrobial activities against *B. subtilis*, *E. coli*, *S. aureus*, *Penicillium*, *Aspergillus*, *Rhizopus* and *yeast*. And CS/Ag/ZnO blend films had higher antimicrobial activities than CS/Ag and CS/ZnO blend films. Moreover, the blend films almost maintained the initial color of chitosan, which have potential application as antibacterial materials.

1. Introduction

Chitosan is one such polymer with antimicrobial activity, which is the second most plentiful natural biopolymer and has the advantages of biodegradability, biocompatibility and excellent film-forming ability [1–4]. However, as a monocomponent antimicrobial agent, chitosan has been far from meeting requirements for some special conditions. So, hybrid materials that were based on CS with other antibacterial materials have attracted much attention during the last few years. For instance, the combination of inorganic agents Ag, Zn, SiO_2, TiO_2 has been reported [5–10]. Among them, chitosan–Ag nanoparticle composite had significantly high antibacterial activity with the presence of a small content (2.15%, w/w) of Ag NPs in the composite [5]. But the composite suffered from a change in color as a result of high content of Ag, which seriously limited their applications. On the other hand, the antibacterial activities of the composite were not ideal when the content of Ag was low. If there is other white metal oxide that can partly replace Ag and be simultaneously incorporated into the chitosan matrix, it would not only enhance the antibacterial property, but also still maintain the color of the chitosan.

Zinc oxide has attracted wide interest because of its good photocatalytic activity, high stability, antibacterial property and non-toxicity [11–13]. Nevertheless, it is well known that CS is only soluble in aqueous solutions of organic or mineral acids. Zinc oxide reacts easily with acidic substance, and it is difficult to synthesis CS/ZnO composite.

In this study, novel chitosan/Ag/ZnO (CS/Ag/ZnO) blend films with high antibacterial activities were successfully prepared for the first time via a mild one-step method of sol-cast transformation. In this method, Ag NPs were generated by using chitosan as the reducing agent under hot alkaline condition and at the same time ZnO NPs successfully formed in the composite. Especially, the product with low concentration of Ag maintained the initial color, which may have potential application as antimicrobial materials.

2. Experimental and materials

2.1. Materials

Chitosan, with degree of deacetylation of 85.46% and molecular weight of 2.6×10^5, was purchased from Jinan Haidebei Marine Bioengineering Co., Ltd. (China). Zinc oxide, silver nitrate, sodium hydroxide, sodium chloride, sucrose, glucose and acetic acid (>99%) were analytical grade and purchased from Guangdong Xilong Chemical Co., Ltd. Beef extract, peptone and agar powder were bacteriological grade. Potatoes were purchased from the nearby market. *Bacillus subtilis* (*B. subtilis*), *Escherichia coli* (*E. coli*), *Staphylococcus aureus* (*S. aureus*), *Penicillium*, *Aspergillus*, *Rhizopus* and *yeast* were prepared by Microorganism Lab of Xiangtan University. Deionized water was used to prepare for all the solutions in this paper.

* Corresponding author. Tel.: +86 731 58292229; fax: +86 731 58292477.
E-mail address: djcwye@163.com (J.-C. Deng).

1385-8947/$ – see front matter © 2010 Elsevier B.V. All rights reserved.
doi:10.1016/j.cej.2010.03.051

Table 1
The amounts of added ZnO and $AgNO_3$ and mass ratios of Ag and ZnO to CS (the chitosan amount was 1.0 g).

Sample	Added ZnO amount (g)	Added $AgNO_3$ amount (mg)	Mass ratio of ZnO to CS (wt.%)	Mass ratio of Ag to CS (wt.%)
CS-1	0.01	1.6	1	0.1
CS-2	0.03	1.6	3	0.1
CS-3	0.05	1.6	5	0.1
CS-4	0.1	1.6	10	0.1
CS-5	0.01	7.9	1	0.5
CS-6	0.03	7.9	3	0.5
CS-7	0.05	7.9	5	0.5
CS-8	0.1	7.9	10	0.5
CS-9	0	1.6	0	0.1
CS-10	0.1	0	10	0

2.2. Preparation

Appropriate amounts of $AgNO_3$ and ZnO powders were dissolved in 100 mL of 1% (v/v) acetic acid to obtain silver and zinc cations. And 1.0 g of chitosan was added to the above solution. Then the mixture was sonicated for 30 min after magnetic stirring and then adjusted acidity by 0.1 M NaOH solution (pH 4.8) to obtain the clear sol. The resulting sol was cast onto glass plates and the transparent films were obtained after solvent evaporating slowly in air. Lastly the transparent films with glass were immersed in 0.1 M NaOH solution for 12 h at 333 K. After being removed from the glass plates, CS/Ag/ZnO blend films were obtained through sufficiently washing with deionized water and drying in an infrared oven. The amounts of added ZnO and $AgNO_3$ and mass ratios of Ag and ZnO to CS were shown in Table 1.

2.3. Characterization

The structure of the blend films was measured using UV–vis spectrophotometer (UV-2450, Shimadzu, Japan) and X-ray diffractometer (D 8 Advance, BRUKER, Germany) of Cu Kα ($\lambda = 0.15406$ nm) radiation in the 2θ ranging from 5° to 80°. The pure CS film and CS/Ag/ZnO blend films with approximately 20-μm thickness were prepared for the XRD test. The morphologies of the films were studied using HITHACH-4300 scanning electron microscope (Japan Electronic Company, Japan) equipped with EDX elemental composition analyzer. The dried samples were freeze-fractured in the liquid nitrogen and then coated with gold before observing. TEM was carried out using FEI TECNAI G2 20 TEM operating at 200 kV.

2.4. Antimicrobial activities

The agar plate method was taken to evaluate the antimicrobial activities of chitosan/Ag blend films and chitosan/Ag/ZnO blend films, compared with the positive control and pure chitosan film [14]. The antimicrobial activities of the films were tested against seven strains of microorganism, i.e., *B. subtilis*, *E. coli*, *S. aureus*, *Penicillium*, *Aspergillus*, *Rhizopus* and *yeast*. The culture of each microorganism was diluted by sterile distilled water to 10^7 to 10^8 CFU/mL. A loop of each suspension was inoculated on nutrient plates with the sample films spread (size: 2 cm × 2 cm). Then the plates with bacteria and fungus were incubated under light at 310 K for 72 h and at 301 K for 48 h, respectively. A corresponding plate without any films was used as a positive control. Especially, antimicrobial test of CS-4, CS-9 and CS-10 in the dark was taken to provide useful data for synergistic effects of Ag and ZnO NPs. Finally, the antimicrobial activities of the samples were evaluated by the diameter of the test microorganism. All the experiments were repeated five times. The results were averaged.

3. Result and discussion

3.1. XRD analysis

Fig. 1 depicts the X-ray diffraction patterns of pure CS film and CS/Ag/ZnO blend films. Two crystal forms existed in pure CS film (Fig. 1a): form I and form II depicted the major crystalline peaks at 10.2° and 19.9°, respectively [15]. However, these two main peaks (Fig. 1b) of CS at 10.3° and 20.3° were affected by doping Ag and ZnO. This indicated that the incorporation of Ag and ZnO particles disrupted the regular order of polymer chains [9]. Compared with Fig. 1a, the diffraction pattern of the CS/Ag/ZnO blend films exhibited six additional peaks at 31.9°, 34.6°, 36.4°, 56.8°, 62.9° and 68.2° (Fig. 1b), which were assigned to the (1 0 0), (0 0 2), (1 0 1), (1 1 0), (1 0 3) and (1 1 2) planes of hexagonal zinc oxide (JCPDS No. 36-1451). Besides, the peak at 38.3° indicated the presence of Ag as shown in Fig. 1b. These data revealed the formation of Ag and ZnO in blend films by the method of sol-cast transformation.

3.2. UV–vis analysis

Fig. 2 presents UV–vis absorbance spectra of pure CS film and CS/Ag/ZnO blend films. As shown in Fig. 2a, the absorption peak of pure CS membrane was not obvious in that there were not conjugated double bonds in the CS molecules. Compared with pure CS film, CS/Ag/ZnO blend films showed two absorption bands (Fig. 2b). One absorption band at 343 nm in Fig. 2b was attributed to the presence of ZnO. Compared with that of the macrocrystalline ZnO

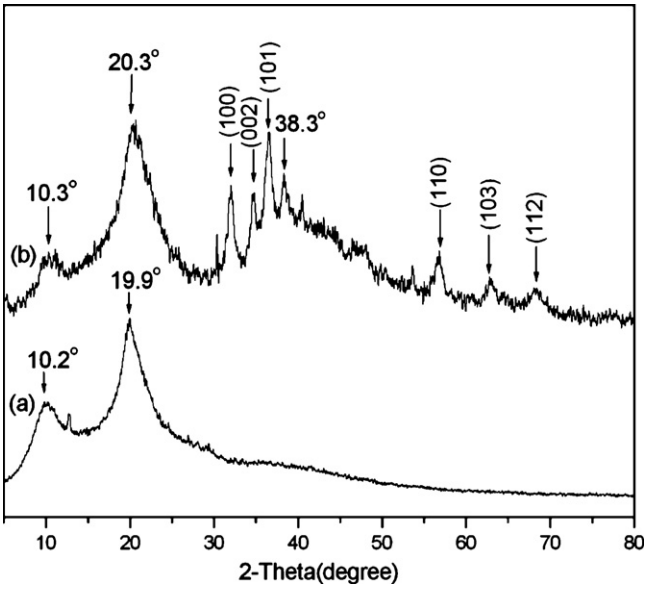

Fig. 1. X-ray diffraction patterns of the samples: (a) pure CS film and (b) CS/Ag/ZnO blend films with 0.5 wt.% Ag and 10 wt.% ZnO.

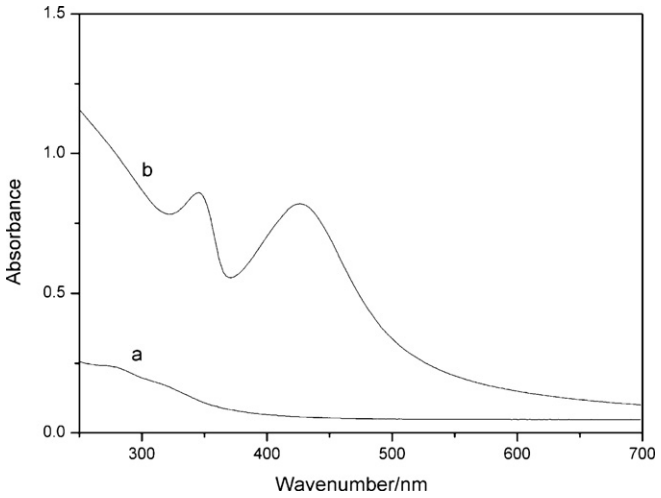

Fig. 2. UV–vis spectra of the samples: (a) pure CS film and (b) CS/Ag/ZnO blend films with 0.5 wt.% Ag and 10 wt.% ZnO.

(about 372 nm) [16], it blue-shifted by 29 nm. This indicated that ZnO within chitosan was in the size of nanometer, which was consistent with the SEM analysis. The other absorption band at about 425 nm was due to the presence of silver NPs [17]. Therefore, it further identified Ag and ZnO generated within chitosan, which agreed well with the above analysis.

3.3. The mechanism of ZnO and silver generation

Chitosan, zinc oxide and silver nitrate were dissolved in dilute acidic solvent. Through adjusting acidity of the solution, the sol containing Zn^{2+} and Ag^{+} ions was obtained. The –OH and $–NH_2$ groups of CS chain reduced Ag^{+} ions to Ag under hot alkaline condition [8]. The possible reactions of the reduction of Ag^{+} to Ag by the chitosan in hot alkaline solution took place as follows:

$$AgNO_3 + aq.CS \rightarrow Ag^{+} + CS \xrightarrow{OH^{-},\Delta} Ag^{0}/CS \quad (1)$$

In order to make Zn^{2+} ions transform into ZnO, the films were immersed in dilute alkaline solution at 333 K. The possible reactions of ZnO formation in hot alkaline solution took place as follows [18–20]:

$$Zn^{2+} + OH^{-} \rightleftarrows Zn\text{-}O\text{-}H^{+} \quad (2)$$

$$Zn\text{-}O\text{-}H^{+} + OH^{-} \xrightarrow{\Delta} ZnO + H_2O \quad (3)$$

Since Zn^{2+} disperses homogeneously in chitosan sol, ZnO was generated homogeneously within chitosan polymer.

3.4. Surface morphologies of the blend films

Fig. 3 presents surface and cross-section SEM photographs of pure CS film and CS/Ag/ZnO blend films. The pure chitosan film displayed a smooth surface (Fig. 3a). With doping Ag and ZnO, the surface of blend films became uneven and studded dense granule (Fig. 3b). As shown in Fig. 3c, Ag and ZnO NPs were observed and the

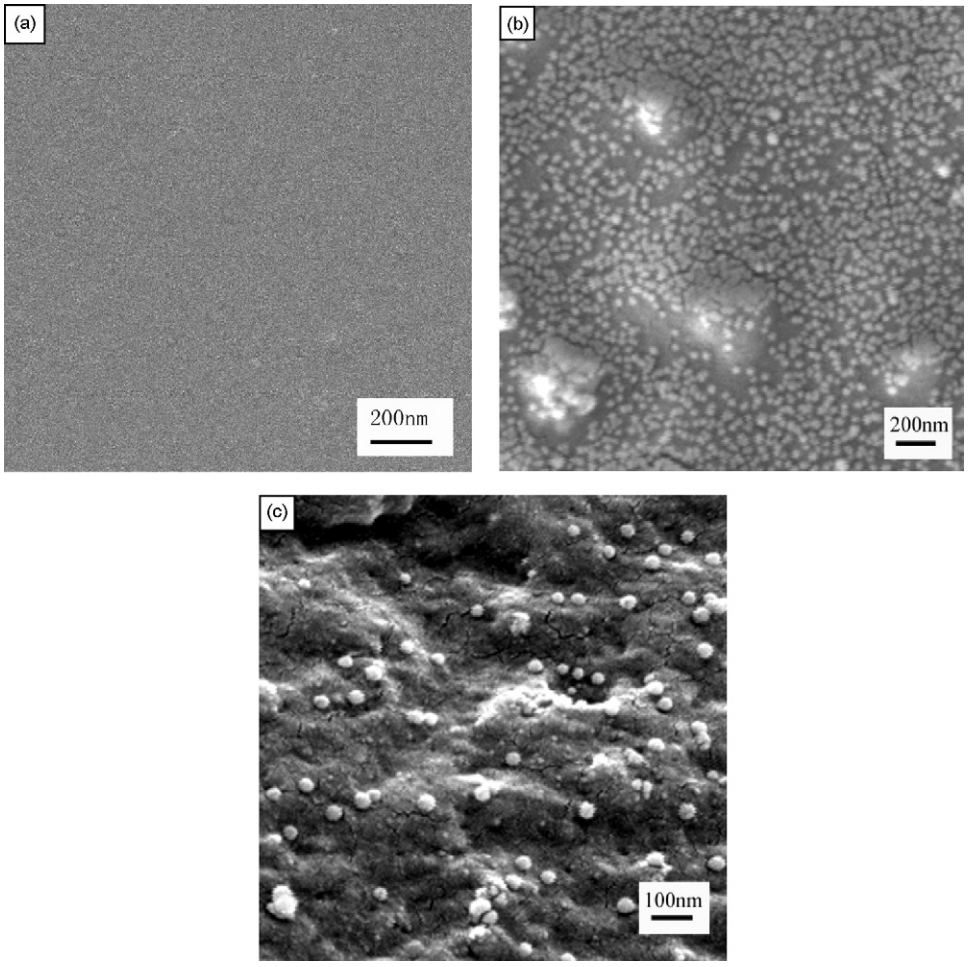

Fig. 3. Surface (a, b) and cross-section (c) SEM photographs of the samples: (a) pure CS film and (b, c) CS/Ag/ZnO blend films with 0.1 wt.% Ag and 10 wt.% ZnO.

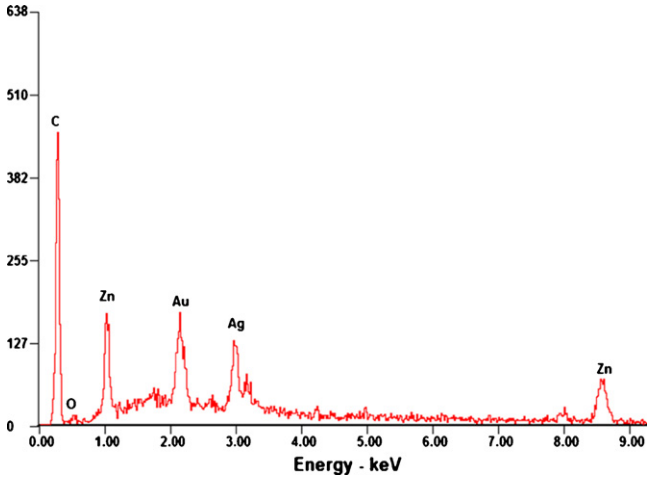

Fig. 4. EDX spectrum of CS/Ag/ZnO blend films with 5 wt.% Ag and 10 wt.% ZnO.

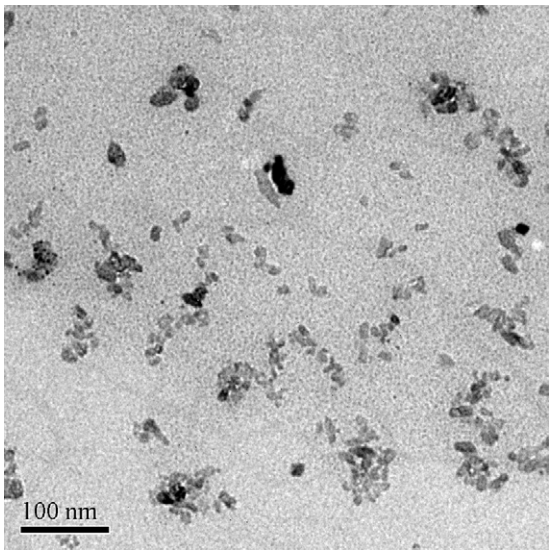

Fig. 5. TEM photograph of CS/Ag/ZnO blend films with 0.1 wt.% Ag and 10 wt.% ZnO after being treated by acid solvent.

particle size was in the range of 10–70 nm. Moreover, the particles had uniform distribution within chitosan polymer.

Because the Ag content in the chitosan/Ag/ZnO blend films was lower beyond the detection limit of EDX and Ag signals and the signals of noise coexisted, it only indicated the presence of Ag qualitatively. If the Ag content was increased, Ag signals could be detected. Thereby, CS/Ag/ZnO blend films with 5 wt.% Ag and 10 wt.% ZnO were prepared by the same method. Fig. 4 illustrates the EDX spectrum of CS/Ag/ZnO blend films with 5 wt.% Ag and 10 wt.% ZnO. As shown in Fig. 4, that C, Zn, O and Ag elements were identified. This result agreed well with XRD analysis.

Fig. 5 depicts TEM photograph of CS/Ag/ZnO blend films that were prepared in dark. Samples for inspection by TEM were prepared by dissolving in 1% acetic acid and coating onto a copper TEM grid. CS and ZnO were dissolved after being treated by acetic acid. As observed in Fig. 5, the nanoparticles were Ag NPs, which were small granular and had a uniform distribution. And the particle size was typically in the range of 10–20 nm.

3.5. Antimicrobial activities

Table 2 presents the diameters of the bacteria colonies on pure CS film and CS/Ag/ZnO blend films with different mass ratios of Ag and ZnO to CS under light. As shown in Table 2, with the increase of Ag and ZnO contents, the diameter (D) of *B. subtilis*, *E. coli*, *S. aureus*, *Penicillium*, *Aspergillus*, *Rhizopus* and *yeast* colonies decreased gradually. However, CS/Ag/ZnO blend films were not as effective at inhibiting the growth of *Aspergillus* as at inhibiting the growth of other microorganism.

The antimicrobial mechanism of chitosan was attributed to interaction with the strongly electronegative microbial surface [21]. CS with doping Ag and ZnO depicted the enhanced antibacterial property due to the photocatalysis and metal release process [10,22–26]. When ZnO NPs (E_g = 3.37 eV) were under light irradiation, electron–hole pairs were generated. The hole (h^+) reacted with OH^- on the surface of NPs, generating hydroxyl radicals ($OH^\bullet$), superoxide anion (O_2^-) and perhydroxyl radicals ($HO_2^\bullet$). These highly active free radicals damaged the cells of microorganism as a result of decomposition and completely destruction [27,28].

As shown in Table 2, under the condition of doping the same contents of Ag and ZnO, CS/Ag/ZnO blend films presented much higher antimicrobial properties than CS/Ag blend films and CS/ZnO blend films. Table 3 shows the diameters of the bacteria colonies on CS-4, CS-9 and CS-10 in the dark. As shown in Tables 2 and 3, the antimicrobial properties of blend films in the dark were not as good as those under light. These phenomena were explained as follows: the presence of transition metals Ag improved the charge transfer, reduced the chance of electron–hole pairs to recombine and promoted the generations of perhydroxyl radicals and other strong oxidizing materials [29,30]. Therefore, the presence of Ag and ZnO enhanced antimicrobial ability of chitosan significantly.

Among all the samples, the CS-8 sample (CS/Ag/ZnO blend films with 0.5 wt.% Ag and 10 wt.% ZnO) showed excellent antimicrobial activities. But considering the color of blend films and the toxicity of silver metal, the CS-8 sample was not perfect for

Table 2
The diameters of the bacteria colonies on pure CS film and CS/Ag/ZnO blend films with different mass ratios of Ag and ZnO to CS under light.

Sample	*D* (mm)						
	S. aureus	*E. coli*	*B. subtilis*	*Penicillium*	*Aspergillus*	*Rhizopus*	*Yeast*
Positive control	18.5 ± 0.2	16.8 ± 0.2	14.8 ± 0.2	10.5 ± 0.2	31.0 ± 0.4	70.0 ± 0.9	10.0 ± 0.2
CS	3.6 ± 0.1	12.0 ± 0.2	6.5 ± 0.2	6.0 ± 0.1	32.0 ± 0.4	70.0 ± 0.8	5.0 ± 0.2
CS-1	2.5 ± 0.1	4.0 ± 0.1	3.8 ± 0.2	4.2 ± 0.2	30.7 ± 0.3	70.0 ± 0.5	4.0 ± 0.2
CS-2	2.5 ± 0.1	2.5 ± 0.1	2.5 ± 0.2	2.0 ± 0.2	25.0 ± 0.3	41.0 ± 0.3	2.6 ± 0.2
CS-3	2.2 ± 0.1	2.0 ± 0.1	2.0 ± 0.1	1.8 ± 0.1	24.0 ± 0.5	0	0.8 ± 0.1
CS-4	0	0	0	1.5 ± 0.1	16.0 ± 0.2	0	0
CS-5	0	0	0	0	15.5 ± 0.1	0	0
CS-6	0	0	0	0	9.6 ± 0.2	0	0
CS-7	0	0	0	0	7.0 ± 0.2	0	0
CS-8	0	0	0	0	3.4 ± 0.1	0	0
CS-9	6.1 ± 0.2	14.0 ± 0.3	8.3 ± 0.2	8.5 ± 0.2	15.7 ± 0.4	21.4 ± 0.2	2.3 ± 0.1
CS-10	4.2 ± 0.2	6.3 ± 0.1	2.6 ± 0.2	9.6 ± 0.3	23.7 ± 0.3	55.1 ± 0.3	8.3 ± 0.2

Table 3
The diameters of the bacteria colonies on CS-4, CS-9 and CS-10 in the dark.

Sample	*D* (mm)						
	S. aureus	*E. coli*	*B. subtilis*	*Penicillium*	*Aspergillus*	*Rhizopus*	*Yeast*
Positive control	17.8 ± 0.23	16.1 ± 0.2	15.2 ± 0.2	10.8 ± 0.2	33.0	70.0 ± 0.7	9.5 ± 0.2
CS	3.4 ± 0.2	11.7 ± 0.1	6.5 ± 0.1	6.3 ± 0.2	31.8	70.0 ± 0.6	5.2 ± 0.1
CS-4	2.0 ± 0.2	8.5 ± 0.1	5.4 ± 0.1	3.5 ± 0.1	25.8 ± 0.1	48.1 ± 0.2	4.0 ± 0.1
CS-9	9.5 ± 0.3	15.8 ± 0.2	15.3 ± 0.2	9.2 ± 0.2	23.0 ± 0.2	52.4 ± 0.2	5.8 ± 0.1
CS-10	13.2 ± 0.2	15.0 ± 0.2	13.6 ± 0.1	9.8 ± 0.2	28.7 ± 0.3	68.5 ± 0.5	8.9 ± 0.2

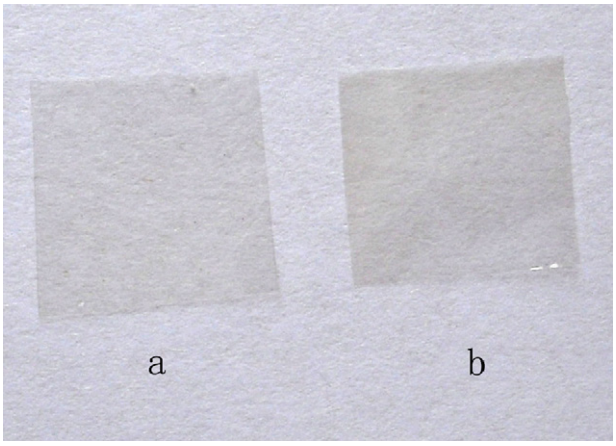

Fig. 6. The optical images of the samples: (a) pure CS film and (b) CS/Ag/ZnO blend films with 0.1 wt.% Ag and 10 wt.% ZnO.

the further applications. By contrast, the CS-4 sample (CS/Ag/ZnO blend films with 0.1 wt.% Ag and 10 wt.% ZnO) also exhibited high antimicrobial activities and translucent appearance (as shown in Fig. 6), indicating a better potential in medical and food packaging fields.

4. Conclusion

Novel chitosan/Ag/ZnO blend films were prepared via the method of sol-cast transformation. Ag and ZnO NPs with spherical and granular morphology had uniform distribution within chitosan polymer. The test of antimicrobial activities showed that CS/Ag/ZnO blend films had higher antimicrobial activities than CS/Ag and CS/ZnO blend films, indicating that the composite of Ag and ZnO enhanced the antimicrobial activities of chitosan. Moreover, CS/Ag/ZnO blend films showed a wide spectrum of effective antimicrobial activities. Especially, the blend films with 0.1 wt.% Ag and 10 wt.% ZnO exhibited high antimicrobial activities and translucent appearance. It suggested that CS/Ag/ZnO blend films had potential application in medical and food packaging fields.

References

[1] S. Hirano, Chitin biotechnology applications, Biotechnol. Annu. Rev. 2 (1996) 237–258.
[2] P. Giunchedi, I. Genta, B. Conti, R.A.A. Muzzarelli, U. Conte, Preparation and characterization of ampicillin loaded methylpyrrolidinone chitosan and chitosan microspheres, Biomaterials 19 (1998) 157–161.
[3] S.-G. Hu, C.-H. Jou, M.C. Yang, Protein adsorption, fibroblast activity and antibacterial properties of poly(3-hydroxybutyric acid-*co*-3-hydroxyvaleric acid) grafted with chitosan and chitooligosaccharide after immobilized with hyaluronic acid, Biomaterials 24 (2003) 2685–2693.
[4] R.A.A. Muzzarelli, C. Muzzarelli, R. Tarsi, M. Miliani, F. Gabbanelli, M. Cartolari, Fungistatic activity of modified chitosans against *Saprolegnia parasitica*, Biomacromolecules 2 (2001) 165–169.
[5] P. Sanpui, A. Murugadoss, P.V.D. Prasad, S.S. Ghosh, A. Chattopadhyay, The antibacterial properties of a novel chitosan–Ag-nanoparticle composite, Int. J. Food Microbiol. 124 (2008) 142–146.
[6] M. Niu, X. Liu, J. Dai, H. Jia, L. Wei, B. Xu, Antibacterial activity of chitosan coated Ag-loaded nano-SiO_2 composites, Carbohydr. Polym. 78 (2009) 54–59.
[7] H. Penchev, D. Paneva, N. Manolova, I. Rashkov, Electrospun hybrid nanofibers based on chitosan or N-carboxyethylchitosan and silver nanoparticles, Macromol. Biosci. 9 (2009) 884–894.
[8] A. Murugadoss, A. Chattopadhyay, A 'green' chitosan–silver nanoparticles composite as a heterogeneous as well as micro-heterogeneous catalyst, Nanotechnology 19 (2008), 015603/1–015603/9.
[9] Z.F. Dong, Y.M. Du, L.H. Fan, Y. Wen, H. Liu, X.H. Wang, Preparation and properties of chitosan/gelatin/nano-TiO_2 ternary composite films, J. Funct. Polym. 17 (2004) 61–66.
[10] X.H. Wang, Y.M. Du, H. Liu, Preparation, characterization and antimicrobial activity of chitosan-Zn complex, Carbohydr. Polym. 56 (2004) 21–26.
[11] M.L. Cohen, The theory of real materials, Annu. Rev. Mater. Sci. 30 (2000) 1–26.
[12] Z.L. Wang, Zinc oxide nanostructures: growth, properties and applications, J. Phys.: Condens. Matter 16 (2004) R829–R858.
[13] A. Sharma, P. Rao, R.P. Mathur, S.C. Ameta, Photocatalytic reactions of xylidine ponceau on semiconducting zinc oxide powder, J. Photochem. Photobiol. A 86 (1995) 197–200.
[14] T.G. Pridham, L.A. Lindenfelser, O.L. Shotwell, F.H. Stodola, R.G. Benedict, C. Foley, R.W. Jackson, W.J. Zaumeyer, W.H. Preston, J.W. Mitchell, Antibiotics against plant disease. I. Laboratory and greenhouse survey, Phytopathology 46 (1956) 568–575.
[15] R.J. Samuels, Solid state characterization of the structure of chitosan films, J. Polym. Sci.: Polym. Phys. Ed. 19 (1981) 1081–1105.
[16] M. Haase, H. Weller, A. Henglein, Photochemistry and radiation chemistry of colloidal semiconductors. 23. Electron storage on ZnO particles and size quantization, J. Phys. Chem. 92 (1988) 482–487.
[17] H.Z. Huang, Q. Yuan, X.R. Yang, Preparation and characterization of metal-chitosan nanocomposites, Colloids Surf. B 39 (2004) 31–37.
[18] D.D. Perrin, The hydrolysis of metal ions. Part III. Zinc, J. Chem. Soc. (1962) 4500–4502.
[19] L. Spanhel, M.A. Anderson, Semiconductor clusters in the sol–gel process: quantized aggregation, gelation, and crystal growth in concentrated ZnO colloids, J. Am. Chem. Soc. 113 (1991) 2826–2833.
[20] S. Sepulveda-Guzman, B. Reeja-Jayan, E. de la Rosa, A. Torres-Castro, V. Gonzalez-Gonzalez, M. Jose-Yacaman, Synthesis of assembled ZnO structures by precipitation method in aqueous media, Mater. Chem. Phys. 115 (2009) 172–178.
[21] S.W. Fang, C.F. Li, D.Y.C. Shih, Antifungal activity of chitosan and its preservative effect on low-sugar candied kumquat, J. Food Prot. 57 (1994) 136–140.
[22] Y. Inoue, Y. Kanzaki, The mechanism of antibacterial activity of silver-loaded zeolite, J. Inorg. Biochem. 67 (1997) 377.
[23] A. Bacchi, M. Carcelli, P. Pelagatti, C. Pelizzi, G. Pelizzi, F. Zani, Antimicrobial and mutagenic activity of some carbono- and thiocarbonohydrazone ligands and their copper(II), iron(II) and zinc(II) complexes, J. Inorg. Biochem. 75 (1999) 123–133.
[24] Z.H. Yang, C.S. Xie, X.P. Xia, S.Z. Cai, Zn^{2+} release behavior and surface characteristics of Zn/LDPE nanocomposites and ZnO/LDPE nanocomposites in simulated uterine solution, J. Mater. Sci. Mater. Med. 19 (2008) 3319–3326.
[25] E.P. Azevedo, T.D.P. Saldanha, M.V.M. Navarro, A.C. Medeiros, M.F. Ginani, F.N. Raffin, Mechanical properties and release studies of chitosan films impregnated with silver sulfadiazine, J. Appl. Polym. Sci. 102 (2006) 3462–3470.
[26] Y.M. Qin, C.J. Zhu, J. Chen, Y.Z. Chen, C. Zhang, The absorption and release of silver and zinc ions by chitosan fibers, J. Appl. Polym. Sci. 101 (2006) 766–771.
[27] Y. Kikuchi, K. Sunada, T. Iyoda, K. Hashimoto, A. Fujishima, Photocatalytic bactericidal effect of TiO_2 thin films: dynamic view of the active oxygen species responsible for the effect, J. Photochem. Photobiol. A 106 (1997) 51–56.
[28] B. Halliwell, J.M.C. Gutteridge, Oxygen toxicity, oxygen radicals, transition metals and disease, Biochem. J. 219 (1984) 1–14.
[29] A. Sclafani, M. Mozzanega, P. Pichat, Effect of silver deposits on the photocatalytic activity of titanium dioxide samples for the dehydrogenation or oxidation of 2-propanol, J. Photochem. Photobiol. A 59 (1991) 181–189.
[30] G. Zhou, J.C. Deng, Preparation and photocatalytic performance of Ag/ZnO nanocomposites, Mater. Sci. Semicond. Process. 10 (2007) 90–96.